Tunnelling and Underground Space Technology 110 (2021) 103745

Contents lists available at ScienceDirect

Tunnelling and Underground Space Technology incorporating Trenchless Technology Research

journal homepage: www.elsevier.com/locate/tust

Augmented satellite InSAR for assessing short-term and long-term surface deformation due to shield tunnelling

Kristina J. Reinders [a,*], Ramon F. Hanssen [a], Freek J. van Leijen [a], Mandy Korff [a,b]

[a] Delft University of Technology, 2628 CN Delft, the Netherlands
[b] Deltares, P.O. Box 177, 2600 MH Delft, the Netherlands

ARTICLE INFO

Keywords:
Ground deformations
InSAR
Long time series
Monitoring
Settlements
Tunnelling

ABSTRACT

In this work, we investigate if, when, and how satellite InSAR can be used for evaluating surface settlements that occur during shield tunnelling in soft soil areas. We evaluate the applicability of InSAR prior, during, and after tunnel construction. Special emphasis is placed on the influence of the InSAR phase ambiguities in relation to short-term settlements that may occur during tunnel construction. We demonstrate that a rough analytic settlement prediction can be sufficient to resolve the most probable phase ambiguity level, leading to an augmented implementation of InSAR. We use the shield tunnel of the in North/South Metro Line Amsterdam as a case study, where surface levelling data is available to assess and validate the results. We conclude that InSAR is a valuable complementary source of information as it provides data outside the area of the conventional surveying benchmarks and it reveals relevant information about settlement patterns before and after traditional construction monitoring periods.

1. Introduction

During the past decades, satellite radar imaging using the Interferometric Synthetic Aperture Radar (InSAR) technique was used to monitor displacements of the land surface (Hanssen, 2001; Özer et al., 2018; Gabriel et al., 1989; Ferretti et al., 2001; Crosetto et al., 2016). The applicability of InSAR was also demonstrated in some tunnel projects (Bischoff et al., 2019; Giardina et al., 2019; Barla et al., 2016; Schindler et al., 2016; Macdonald et al., 2015; Mark et al., 2012; Schneider et al., 2015). This showed that InSAR can be used for (i) the detection of tunnelling-induced settlements, resulting in localization and timing of the settlement, complemented by (ii) an estimation of the quantitative amount of settlement. Particularly for long-term settlements, occurring years to decades after the construction phase ends (Shirlaw, 1995; Mair, 2008; Wongsaroj et al., 2013), InSAR is probably the only economically feasible monitoring option.

The main limitations of InSAR for tunnelling are imposed by the revisit times of the satellites and the condition of coherence—where reflection characteristics of the geo-objects should remain relatively unaltered over time (Hanssen, 2001). Moreover, due to the fixed wavelength of the radar instrument, abrupt changes in the spatial displacement gradients greater than the *wrapping threshold*—defined as a quarter of the physical radar wavelength in the line-of-sight of the radar—may lead to an under- or overestimation of the deformation signal. As surface settlements that occur during excavation of a shield tunnel typically have a magnitude range of a few millimetres to a few centimetres, which may occur within roughly one week of construction at the location where the tunnel boring machine (TBM) has passed (Broere and Festa, 2017), over a spatial distance of a few tens of meters, such deformation ambiguities cannot be ignored in the InSAR estimates. In this paper we extend this analysis and evaluate if, when, and how InSAR can be used in different stages: (i) prior to the tunnel construction, as a design tool to optimise the monitoring plan, (ii) during construction, as a diagnostic tool to detect surface settlements and (iii) after construction as a forensic tool to evaluate damage as a low-cost monitoring tool and to monitor the long-term settlements. We use the twin shield tunnels of the North/South Metro Line in Amsterdam that were excavated in 2011 and 2012 as a case to demonstrate the applicability. Surface settlements larger than or close to the wrapping threshold occurred during this project.

* Corresponding author.
E-mail addresses: k.j.reinders@tudelft.nl (K.J. Reinders), r.f.hanssen@tudelft.nl (R.F. Hanssen), f.j.vanleijen@tudelft.nl (F.J. van Leijen), m.korff@tudelft.nl (M. Korff).

https://doi.org/10.1016/j.tust.2020.103745
Received 25 April 2020; Received in revised form 1 September 2020; Accepted 23 November 2020
Available online 4 January 2021

2. Review and background

This section comprises a short explanation of surface settlements during shield tunneling, the basic concepts of InSAR and the potential of InSAR for tunneling projects.

2.1. Surface Settlement due to tunnelling

During the excavation of shield tunnels surface settlements may occur due to insufficient support at the face, over-excavation, soil relaxation and inefficient tail void filling (Maidl et al., 2013). In practice, the settlements that occur during construction in cross-sectional direction of the tunnel are often calculated with Peck's formula (Peck, 1969) and are well understood. This empirical formula is based on observations and analyses of a large amount of monitoring data from tunnels and is most commonly used for 2D calculations. The settlement trough that occurs in a cross-section perpendicular to the tunnel axis can be expressed by the following Gaussian curve:

$$S(y) = S_{\max}\exp(-\frac{y^2}{2i^2}), \tag{1}$$

where $S(y)$ is the settlement at ground level, y is the horizontal distance from the centreline, $i = 0.28z_0 - 0.1$ is the horizontal distance from inflection point to the tunnel centreline for a sandy soil, as a function of the tunnel depth z_0 (O'Reilly and New, 1982), and $S_{\max}$ is the maximum ground settlement at the tunnel centreline. $S_{\max}$ can be expressed as

$$S_{\max} = \frac{c_L \cdot \pi D_0^2/4}{i \cdot \sqrt{2\pi}}, \tag{2}$$

where the numerator is the product of c_L, the volume loss influence factor—around 0.005 (0.5%) for a slurry machine—and the cross-sectional area of the circular tunnel, scaled by D_0—the outer diameter of the tunnel. The major assumption is that the volume of the settlement trough equals the volume of soil losses around the tunnel. Usually these settlements occur within a length of 40–50 m, which corresponds to typically one week of construction (Broere and Festa, 2017). Fig. 1 shows the development of surface settlement as tunneling progresses.

On the other hand, the long-term settlements of shield tunnels in soft soil conditions are not so well understood and have large uncertainties in their predictions (Mair, 2008; Wongsaroj et al., 2013). These settlements may occur in the years and even decades after construction due to consolidation and creep of clayey soils. Although the magnitude of these settlements can account for 30–90% of the total settlements (Shirlaw, 1995), only a few studies were performed (Stallebrass et al., 1994; Addenbrooke, 1996; Mair, 2008; Shin et al., 2002; Bowers et al., 1996).

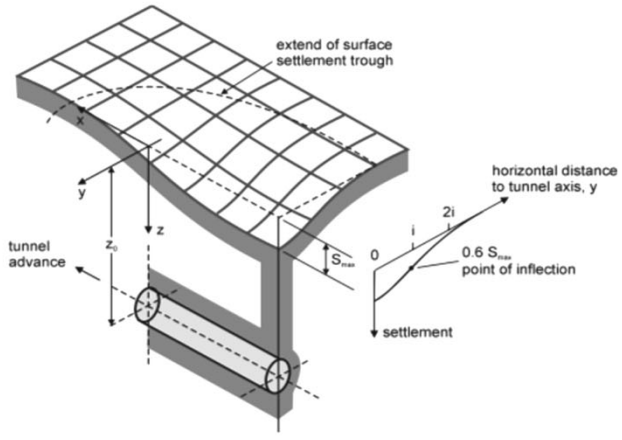

Fig. 1. Three-dimensional representation of surface settlement induced by a tunnel (Attewell et al., 1986).

From these studies it is known that the long-term settlement trough tends to be deeper and wider than the trough that occurs during construction. As traditional monitoring is generally ceased within a year of the end of construction, little data is available on the exact amounts of long-term settlements due to tunnelling in soft soils. This is where InSAR may be of complementary value.

2.2. Basic concepts of InSAR

SAR is a remote sensing technique that can measure displacements of the ground or objects on it (Elachi, 1987). It is an imaging radar, mounted on a satellite, that sends pulses of electromagnetic waves to the earth. Part of these pulses reflect back towards the antenna of the satellite. The phase of the incoming signal, which is dependent on the two-way travel time of the signal, is recorded. Table 1 shows several characteristic elements of current C-band and X-band missions.

A reflection from the ground may stem from two types of scatterers, i.e. distributed scatterers (DS) and point scatterers (PS). PS are pixels which have one dominant reflecting object within the pixel's footprint that shows constant behaviour over time. DS are pixels which contain multiple objects with a weaker reflection but that also show consistent behaviour over time.

A single phase observation φ_M in one SAR acquisition does not contain interpretable information. However, when obtaining a second phase observation φ_P, at a different location, and subsequently repeating those measurements during a second radar acquisition at the next satellite pass, the double-difference (i.e., spatial and temporal phase difference) $\Delta\varphi_{\text{int}}$ between the two measurements can be determined, i.e. the interferometric phase

$$\Delta\varphi_{\text{int}} = (\varphi_M - \varphi_P)_{t_2} - (\varphi_M - \varphi_P)_{t_1}, \tag{3}$$

see Fig. 2. Typically, these differences have a precision in the order of a few millimeters. By calculating the interferometric phase for each successive image, a time series of displacements is obtained. The interpretation of double-difference measurements requires an arbitrary reference point and reference time. The movement of all points within the analysis is relative to this reference point and time. The relation between phase and displacement D is given by

$$\Delta\varphi_{\text{int}} = \frac{2\pi}{\lambda}\cdot 2D = \frac{\pi}{\lambda/4}D \tag{4}$$

where $2D$ is the extra two-way distance between satellite and target, and λ is the radar wavelength, which is typically either 31 or 56 mm for X-band and C-band satellites respectively, cf. Table 1. Thus, a phase change of π radians corresponds with a displacement of $\lambda/4$—a quarter of the physical radar wavelength, in the line of sight direction to the

Table 1
Relevant characteristics for current C-band and X-band SAR missions. The repeat cycle indicates the achievable repeat interval for interferometric combinations. The revisit time indicates how often the area of interest can be imaged, albeit with different viewing gemetries. [1]This is assuming that the satellite is tasked to acquire data over the area of interest. [2]These values reflect situations for latitudes higher than 45 degrees.

Mission	Band	wavelength (mm)	wrapping threshold (mm)	Repeat cycle[1] (days)	Revisit time[1,2] (days)
RadarSAT-2	C	56	14	24	6
TerraSAR-X/ Tandem-X/ Paz	X	31	7.8	11	4
Cosmo-Skymed 1/ 2/3/4	X	31	7.8	4	2
Sentinel-1 a/ b	C	56	14	6	2

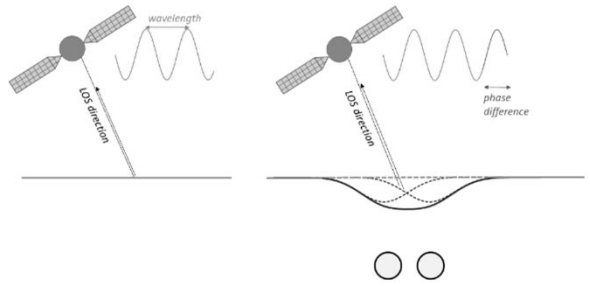

Fig. 2. Two sequential InSAR measurement before and after deformation due to tunnel construction (after Özer et al., 2019). The LOS is the line of sight direction of the radar signal.

radar.

If a pixel has displaced more than π radians, a multiple of 2π should be added or subtracted from the interferometric phase to get the correct absolute phase change

$$\psi = \Delta\varphi_{\text{int}} + 2\pi k, \quad k \in \mathbb{Z}, \tag{5}$$

where k is the integer cycle correction, or the phase ambiguity number. This procedure of ambiguity resolution is called phase unwrapping. Erroneous phase ambiguities are easily detectable in case the deformation rates are constant and small. However, if the settlements are close to or larger than the wrapping threshold $\lambda/4$, i.e. 7 or 14 mm, the InSAR result may yield an erroneous ambiguity number. Fig. 3 shows an example of an InSAR time series. Observation *A* is positioned around the wrapping threshold and may be estimated with ambiguous phase levels, leading to different (ambiguous) solutions.

To overcome this problem, prior assumptions about the deformation behaviour are required. For example, if we expect that the ground surface will behave similar in the future as in the past, we would select the middle ambiguity level in Fig. 3. On the other hand, if we expect sudden settlements due to underground tunnelling works, occurring at the time of observation *A*, the lower ambiguity level seems more likely. And if we would expect heave at the time of observation *A*, the upper ambiguity level might be the correct choice. This example demonstrates that a priori knowledge is required to estimate the correct ambiguity level.

2.3. Value assessment of InSAR for tunneling

To evaluate the potential and overall feasibility of InSAR for tunnelling we can distinguish a specific value before, during, and after construction.

Prior to tunnel construction, InSAR can be used (i) to understand the (undisturbed) stability of the area of interest, by evaluating the archive of satellite data, and (ii) to determine the position and distribution of coherent measurement points, which serves as a design tool to complement these with the in situ surveying network to be installed.

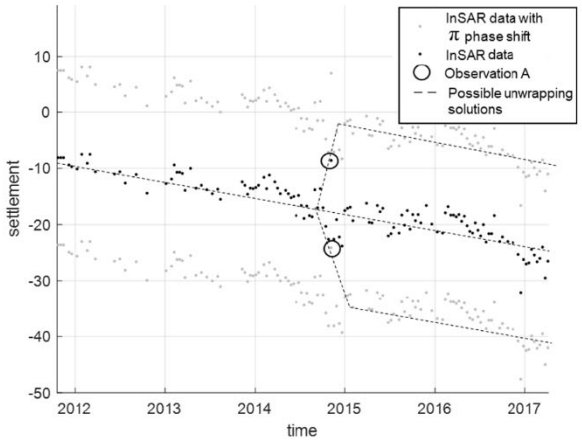

Fig. 3. Potential ambiguity levels, or unwrapping solutions, for an InSAR time series.

In soft soil areas it is common to find a background settlement in the form of long term subsidence mechanisms. As InSAR data is available since decades, it can reveal these spatial and temporal patterns of ground motion over a wide area, prior to construction. This can be used to find the driving mechanisms behind the observed deformation, which is valuable in the risk assessment and the design of the construction phase.

When the influence zone of the tunnel is known, the location, density and quality of coherent InSAR points can be assessed. This analysis can be important for economic reasons, to design the required surveying efforts during and after the construction phase. Apart from a cost-saving driver, inclusion of the information readily available from satellites could lead to optimization of the monitoring plan and improved risk detection thresholds.

During construction, InSAR measurement points can be used complementary to the traditional monitoring, e.g., to assess the displacements of the ground and buildings in an area outside the traditional surface levelling points. This way, the information is used as a diagnostic tool to detect deformations. The value is defined by the range of observable signals, which is case-specific. For a particular situation, potential displacement signals (both intentional as well as unintentional) need to be defined. Ideally, this is done in terms of a model, but also expectations on location, spatial extend, spatial smoothness, temporal extend, temporal smoothness, direction and magnitude are valuable. These so-called signal characteristics can then be evaluated against the spatio-temporal sampling and extend of the InSAR measurements.

Typically, *after* a tunnelling construction project ends, the in situ monitoring network is discontinued. This means that dynamic effects, i.e. displacements, and settlements on the longer term cannot be observed any more. As the magnitude of such long term settlements can account for 30–90% of the total settlements (Shirlaw, 1995), SAR observations are most like the only source of information. A regular evaluation using InSAR is therefore cost-effective and sufficient. Moreover, the InSAR information can be used as a forensic tool to investigate, post hoc, the displacements that may have led to observed damage or failure of a construction.

3. Method

For this study we designed an augmented InSAR method by combining InSAR with prior expert information, and we evaluate the overall feasibility of InSAR for tunneling by addressing how InSAR can be used prior, during, and after construction.

3.1. Prior to construction

Based on the influence zone of the tunnel we first assess the location, density and quality of coherent InSAR points. An evaluation of the InSAR data prior to construction will yield a preliminary quality assessment of the measurements during construction. In turn, this leads to the definition of detectability thresholds, such as the minimal detectable displacements.

Second, we evaluate with InSAR data the deformation patterns prior to construction. This analyses can reveal phenomena in surface deformation prior to tunnel construction and serve as baseline for the future project.

3.2. During construction

To use InSAR during construction as a diagnostic tool to detect deformations, prior information is needed to select the most probable phase ambiguity level. We use the analytic settlement prediction of

(Peck, 1969) as prior information to overcome the problem of ambiguity, following the scheme in Fig. 4.

Then we process the selected InSAR points with three different ambiguity levels and compare them with the measurement of the surface levelling points.

3.3. Assessment of InSAR data after construction

Based on the correct ambiguity level that we have chosen with the prior information during construction, we evaluate the long-term deformation trends, in the years after construction, with InSAR data. Second, we investigate if InSAR information can be used as a forensic tool to investigate, post hoc, the displacements that may have led to observed damage or failure of a construction.

4. Study area: North/South Metro Line, Amsterdam

To evaluate the value of InSAR for a practical situation, we use the case of the shield tunnel of the North/South Metro Line in Amsterdam, which was excavated with a slurry tunnel boring machine. In this section first the location and geology of the study area are described. Second the type of conventional monitoring data and the InSAR data are explained.

4.1. Location

In Amsterdam, a new metro line between Scheldeplein and Centraal Station, the so-called North/South Metro Line, was constructed between 2002 and 2018 in soft soil conditions. The 3.8 km long track consists of twin shield tunnels with a diameter of 6.52 m and has three deep intermediate stations: Ceintuurbaan, Vijzelgracht and Rokin. The tunnels were excavated between 2010 and 2012 with a slurry tunnel boring machine. In this research we focus on the part of the line between Scheldestraat and Ceintuurbaan, see Fig. 5.

In the first part of this trajectory, from Scheldeplein to Cornelis Troostplein, the tubes are located at the same depth next to each other with a spacing of 3.75 m. In the second part, from Cornelis Troostplein to Ceintuurbaan, the tubes are located above each other with 7 m spacing. The depth of the axis along the track varies from 15 to 30 m. The tubes are mostly located in sand or clayey sand. The soil conditions are shown in Fig. 6 and described in the next section in more detail. Both tubes in this trajectory were drilled from south to north with a slurry shield tunnel boring machine (TBM).

We selected two instrumented cross sections: *Churchilllaan* in the first part of the trajectory and *Van Ostadestraat* in the second part of the trajectory, see Fig. 5. The TBM of the West tunnel passed *Churchilllaan* on 27-06-2011 and *Van Ostadestraat* on 01-08-2011. The TBM of the East tunnel passed *Churchilllaan* on 27-01-2012 and *Van Ostadestraat* on 26-02-2012. The West tunnel (numbered with [1] in Fig. 6) was drilled in 2011 and the East tunnel (numbered with [2] in Fig. 6) in 2012.

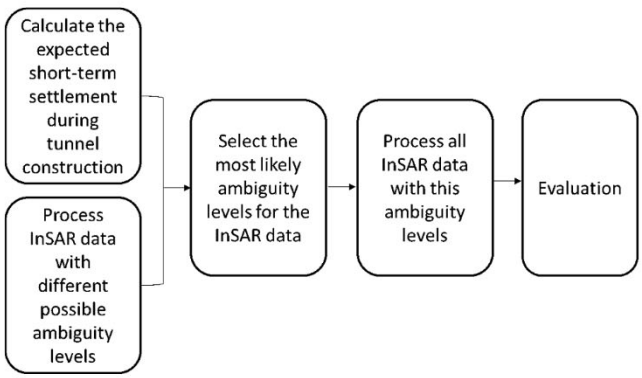

Fig. 4. Flowchart for augmented InSAR data processing prior to construction.

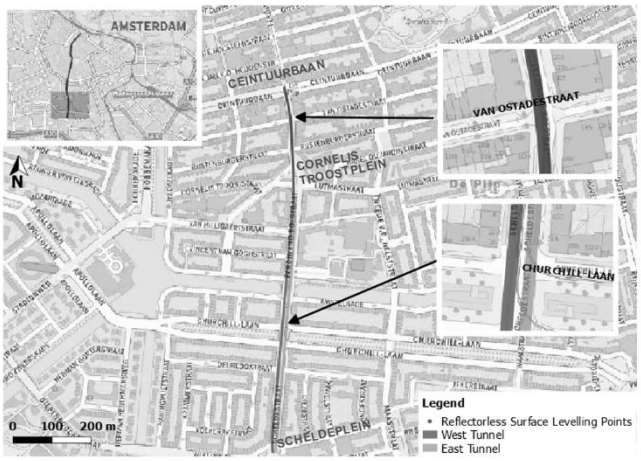

Fig. 5. South part of the track of the North/South Metro Line.

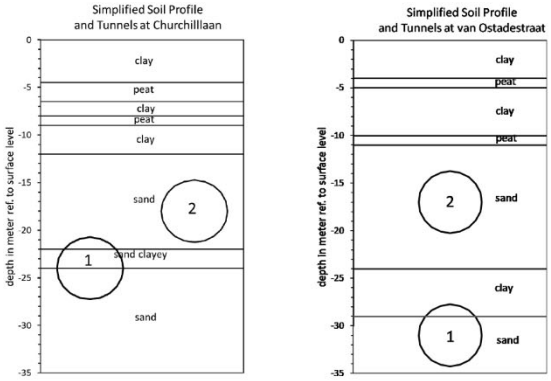

Fig. 6. (a) Simplified soil profile and depth tunnels at *Churchilllaan*. (b) Simplified soil profile and depth tunnels at *Van Ostadestraat*.

4.2. Geology

The geology in the city of Amsterdam consists of a Holocene layer of approximately 10 m to 13 m thickness which consists of clay with peat layers and some sand. The Pleistocene layers, with the first, second and third sand layers, including intermediate clay layers are found below the Holocene to a depth of well over 50 m, see Fig. 7.

4.3. Conventional monitoring data

During the construction of the North-South Line, the buildings and surface in the zone of influence were extensively monitored with 74

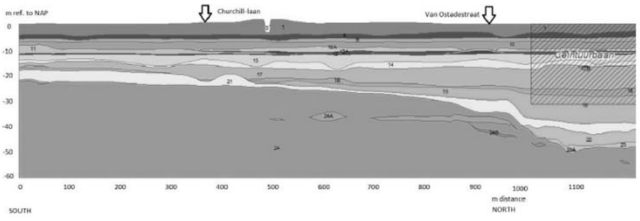

Fig. 7. Geotechnical cross section along the south part of the track of the North/South Metro Line, based on (Adviesbureau Noord/Zuidlijn, 2014). 1 = sand/clay/peat, 8 = peat (Hollandveen), 9 = old marine clay, 10 = wad deposit (sand), 10a = silt, 11 = wad deposit (clay), 12 = peat, 12a = peat (basisveen), 13 = 1st sandlayer, 14 = Alleröd deposit (sandy clay), 17 = 2nd sand layer, 19 = Eem clay, 21 = intermediate sand layer, 24 = 3rd sand layer, 24a = 3rd sand layer, 24b = 3rd sand layer.

robotic total stations (Van der Poel et al., 2006; Cook et al., 2007). On the buildings, prisms were installed that were measured by the total stations (Korff and Mair, 2013). In order to measure the ground settlement, the automatic total stations recorded the vertical heights of points positioned on a virtual horizontal grid without the need for prisms on the surface. This is known as refectorless surface levelling.

In the line of the axis of each tunnel, the surface was measured hourly at one meter intervals. Furthermore, at several locations also points perpendicular to the tunnel axis were measured to obtain a transversal settlement profile. In the detail in Fig. 5 the reflectorless surface levelling points are shown for the *Churchilllaan* and *Van Ostadestraat*.

The monitoring started approximately two months before the TBM passed and ended one month after passing of the TBM. Both the surface and structures in the expected influence zone of the tunnel were extensively monitored. Fig. 8 shows an example of a monitoring time series.

The total stations were linked to each other and were checked on a regular basis against a benchmark of a deep datum, positioned outside the tunnel influence zone, on the stable third sand layer (Cook et al., 2007).

4.4. InSAR data

For the chosen trajectory, we use SAR data acquired between 2009 to 2018 by the TerraSAR-X satellite. Our dataset contained data along the whole tunnel track in a strip of around 100 m wide, i.e. extending approximately 50 m to each side of the tunnels. The data set is acquired from an ascending orbit, where the satellite passes from south to north, and since the antenna is pointing to the right, the radar line of sight direction is roughly west-east. The repeat cycle of the satellite is 11 days and the radar wavelength λ is 31 mm, see Table 1. The displacements are measured in the line of sight to the satellite, with an incidence angle of 32 degrees with respect to zenith. Therefore, the measurements are sensitive to the projection of the 3D displacement onto the line of sight direction. Here we assume that the horizontal displacements are small and therefore we mapped the measured displacement in the vertical direction. This assumption is common for tunnelling conditions as vertical displacements are expected to be more dominant than horizontal.

We use both distributed scatterers (DS) and persistent scatterers (PS) in our research. Since InSAR data is relative both in time and space, a temporal and spatal reference have to be chosen. In the time domain, the first epoch in the displacement time series is set to zero. In the spatial domain, the average deformation rate of the complete dataset over Amsterdam is set to zero. It should be noted that these choices are arbitrary and do not influence the interpretation of the results.

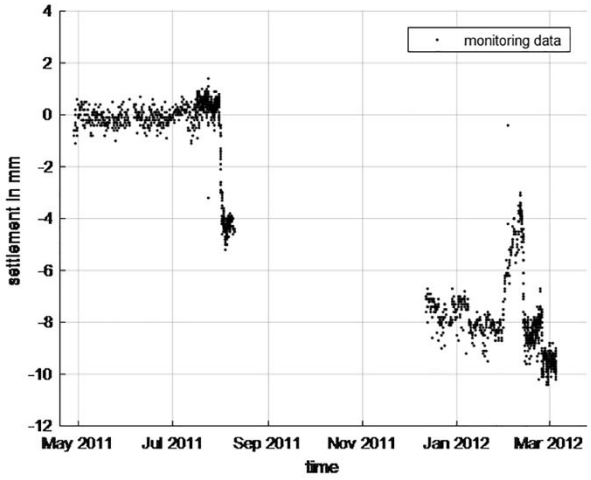

Fig. 8. Example of monitoring of one reflectorless surface levelling point.

5. Data analysis

In the following section we subsequently analyze the InSAR time series data prior, during, and after construction of the North/South Metro Line.

5.1. Assessment of InSAR data prior to construction

First we retrieved the relevant InSAR data is and second we evaluated this data for the period prior to construction.

5.1.1. Retrieving the relevant InSAR data

To reveal the patterns in surface ground motion prior to construction, we use the InSAR data in the zone of influence of the tunnel, which extends up to ~2.5i m to both sides of the tunnels, depending on the depth and soil type (Cording et al.,1976, Attewell et al., 1986), where i is the distance from the tunnel center line to the point of inflection, see Eq. (1). In our case, the tunnel tubes are located at a depth of 18 to 32 m, see Fig. 6, which results in a influence zone of at most 22 m to both sides of the tunnels. Since the InSAR data processing yields estimates of the elevation of the measurement points, see Hanssen (2001), we distinguish points higher and lower than 3 m from the street level, which are linked to the buildings and the ground surface, respectively. The

Fig. 9. InSAR points near *Churchilllaan*: (a) low points, on the ground surface. (b) high points, on the buildings. The colored dots indicate the vertical deformation rates in mm/y. The yellow lines indicate the influence zone of the tunnel.

location precision is at the decimeter level (Dheenathayalan et al., 2016). Fig. 9a is a top view of *Churchilllaan* showing the influence zone and the location of the scatterers on the ground. Fig. 9b shows the location of the scatterers on the buildings. Note, that the results are already projected onto the vertical direction.

5.1.2. Evaluating the data

First, we assess the location and density of the InSAR points. We observe that the point density at the outer limits of the influence zone is large whereas it is low in the middle of the expected settlement trough. This is due to the (to be expected) loss of coherence in the street, where all kinds of (construction) activities take place. Only at cross sections with other streets the point density is sufficient to detect the settlement trough with InSAR.

On the other hand, almost all buildings have coherent scatterers, which remain coherent and can therefore be used to monitor the buildings during and after construction, see Sections 5.2 and 5.3 respectively. Based on the quality of the points, the minimal detectable deformation (MDD) of each point can be established (Chang et al., 2018).

Second, we evaluate the InSAR data prior to construction, based on two selected cross sections. The InSAR data before 2011, i.e. prior to tunnel construction, show different deformation patterns for *Churchilllaan* and *Van Ostadestraat*. In particular, whereas at *Van Ostadestraat*, Fig. 10a, the settlement remains constant, *Churchilllaan* shows a significant change in settlement velocity at the end of 2010, which is *before* tunnel boring commenced, see Fig. 10b. One of the reasons for the change in settlement velocity at *Churchilllaan* could be the construction of two vertical shafts of around 30 m deep that will serve as an emergency exit for the tunnels. See Fig. 11 for the location of the shafts and the location of the InSAR point *X* from Fig. 10b. The shafts were excavated *in the wet* in 2010 by pushing prefabricated concrete rings into the ground and excavating within these concrete rings. After complete excavation, the shafts were pumped dry late 2010, which is around 6 months before tunnel 1 was excavated. This corresponds well to the observed change in settlement velocity in the InSAR data, Fig. 10b. The long-term consequence of the shaft construction can be explained by the drainage effect of the shafts, which act as a vertical well due to the non-zero permeability of the walls. This drainage can cause consolidation of the soil in the years after construction, leading to the observed surface settlements.

We conclude that in our case, the amount of InSAR points was sufficient to reveal spatial and temporal patterns of deformation prior to construction, caused by shaft excavation. This demonstrates that InSAR can be used as a diagnostic tool to detect deformations (or the absense of deformations) before conventional monitoring commences.

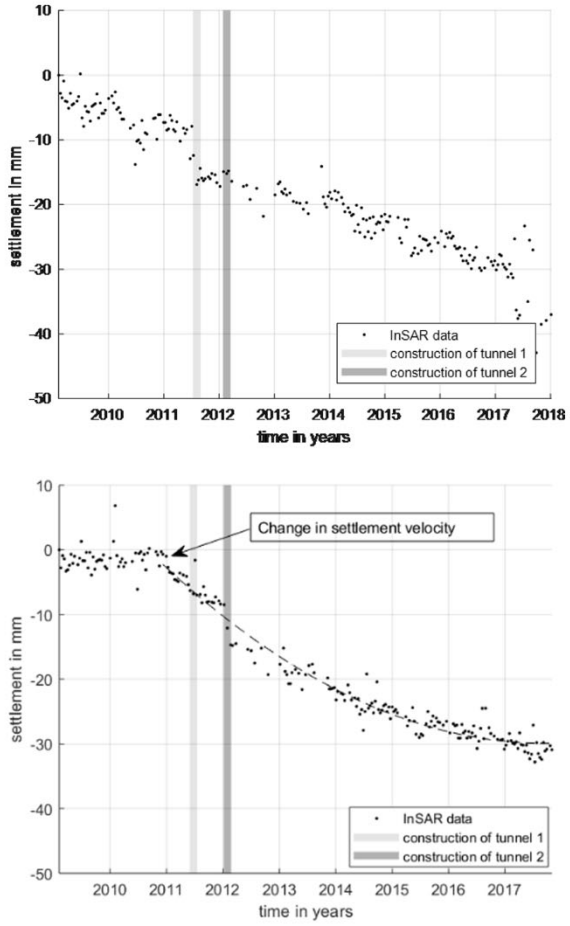

Fig. 10. Vertical settlement (mm) of (a) a point at *Van Ostadestraat*, and (b) point *X* in Fig. 11 at *Churchilllaan*.

5.2. Assessment of InSAR during construction

We compute the expected surface settlements *during* construction and use these priors to guide the selection of the correct InSAR ambiguity levels, followed by an evaluation of the results.

5.2.1. InSAR ambiguity resolution

The revisit time of SAR satellites is typically once every few days or weeks, see Table 1. Thus, in case the displacements between two subsequent InSAR acquisitions are larger than the wrapping threshold $\lambda/4$, an erroneous ambiguity level may be estimated, see Section 2.1. Selection of the correct ambiguity level is only possible given prior information. Here, we use the expected settlement that is calculated before construction as prior information to estimate the most likely ambiguity level.

Based on the soil profile, the depth of the tunnels and the expected a priori volume loss, the expected settlement trough for both cross sections is calculated following Peck (1969). We assume a typical average volume loss of 0.5% during tunnel construction (Vu et al., 2016) and assume that this value has an uncertainty of 0.25 percentage points, which is regarded as the standard deviation of a normal distribution. For tunnel 1 at *Churchilllaan*, this results in a settlement of 10 ± 5 mm, see Fig. 12. Assuming a normal distribution, this implies that the probability of a settlement larger than the wrapping threshold projected onto the vertical, i.e. 9.1 mm, is ~55%, see Fig. 13.

We use the two points on top of the tunnel axis at *Churchilllaan*, see Fig. 14, and process them with the same three different ambiguity levels. Then we compare the ambiguity levels with the expected settlement, see Fig. 15. The upper ambiguity level would represent heave, which has a probability of 2% based on the settlement calculation, and is hence very

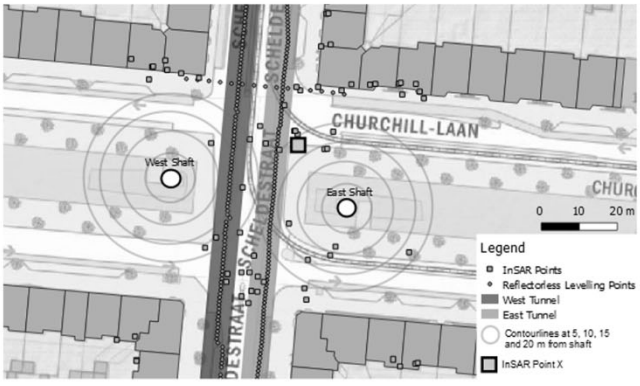

Fig. 11. Location vertical shafts at the *Churchilllaan*. The point *X* is indicated with the blue square, and its time series is shown in Fig. 10.

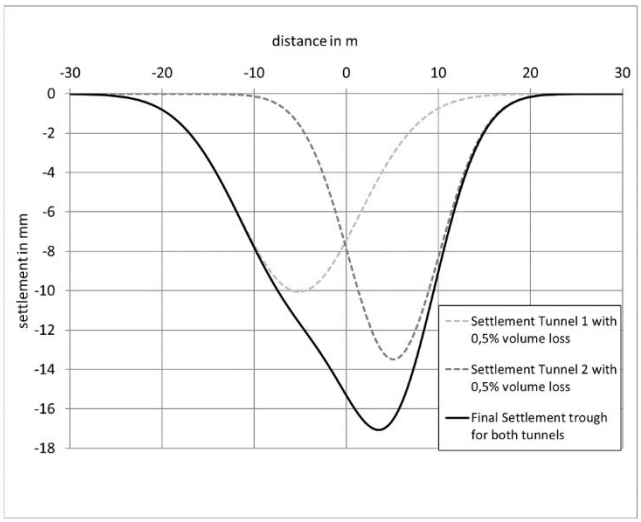

Fig. 12. Settlement trough at *Churchilllaan* with 0.5% volume loss.

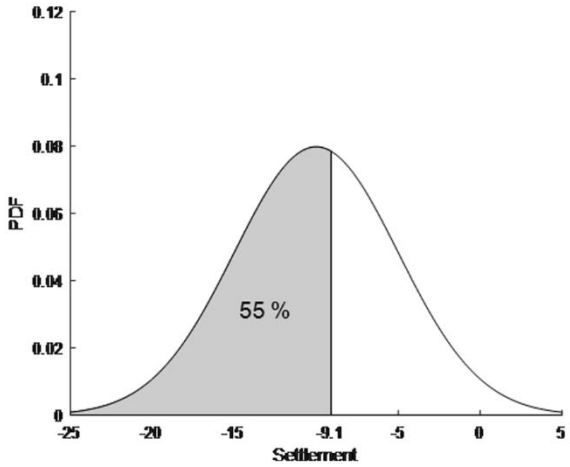

Fig. 13. Probability density function for the maximum settlement of tunnel 1 at *Churchilllaan*.

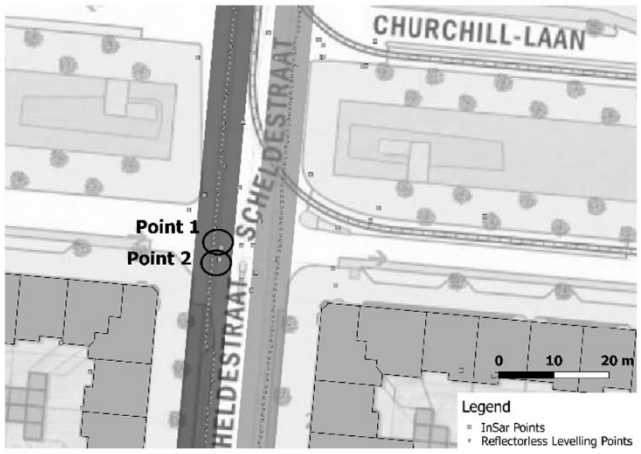

Fig. 14. Surface levelling points and InSAR data points at *Churchilllaan*.

unlikely. The lower ambiguity level shows a settlement of more than 20 mm for *Churchilllaan* which has a probability of less than than 2%. Thus, given this information, the middle ambiguity level, with 8 mm settlement, is considered to be the most likely solution.

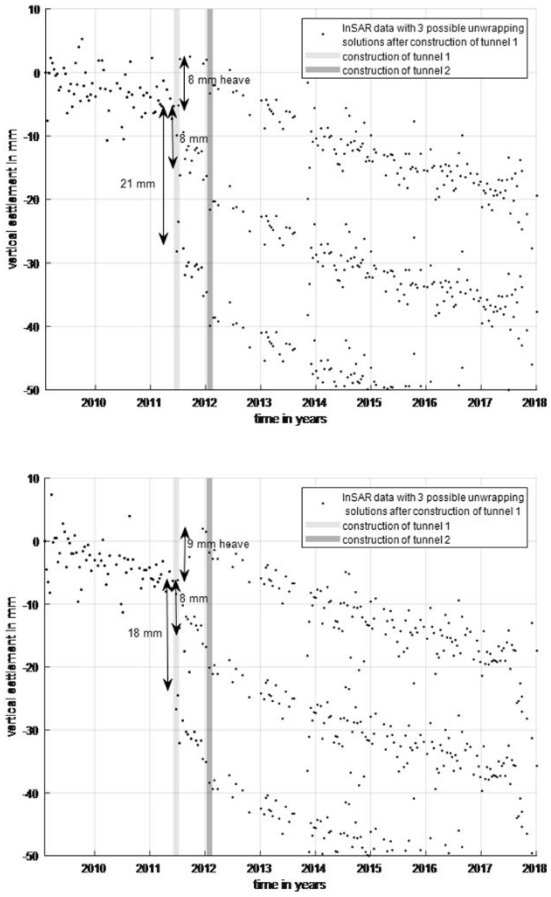

Fig. 15. Three different ambiguity levels at *Churchilllaan*, point 1 (top) and point 2 (bottom).

5.2.2. *Evaluating the results*

Validating the InSAR results (with the selected ambiguity level) with the in situ monitoring data, see Fig. 16, shows a good agreement. Thus, when we can expect surface settlements to be close to, or larger than, the wrapping threshold, prior information is essential to select the correct ambiguity level in InSAR data. It is important to stress that these are differential settlements, i.e., they hold for relative displacements between two points at a particular spatial separation. When the use of an analytic settlement prediction enables the selection of the most probable ambiguity level, we refer to this as an *augmented implementation of InSAR*. Augmented InSAR can be used to evaluate surface settlements at locations were no conventional monitoring is available and it can be used to assess long-term trends, see Section 5.3.

5.3. *Assessment of InSAR after construction*

The same InSAR dataset is used to assess the deformation *after* the construction phase. First, the InSAR ambiguity resolution is assessed, followed by an evaluation of the results.

5.3.1. *InSAR ambiguity resolution*

We select three InSAR points perpendicular to the tunnel axis at *Churchilllaan* and at *Van Ostadestraat*, see Figs. 17 and 18, and select the chosen ambiguity level of Section 5.2. Then we compare these solutions with in situ monitoring data. Figs. 19 and 20 confirm that the chosen ambiguity level was correct.

We then include all InSAR points at the cross section of *Churchilllaan* in our analysis. The dataset now contains 59 points, see Fig. 21. We process these points with the selected ambiguity level and approximate the expected curve, see Eq. (1), locally with a second-degree polynomial.

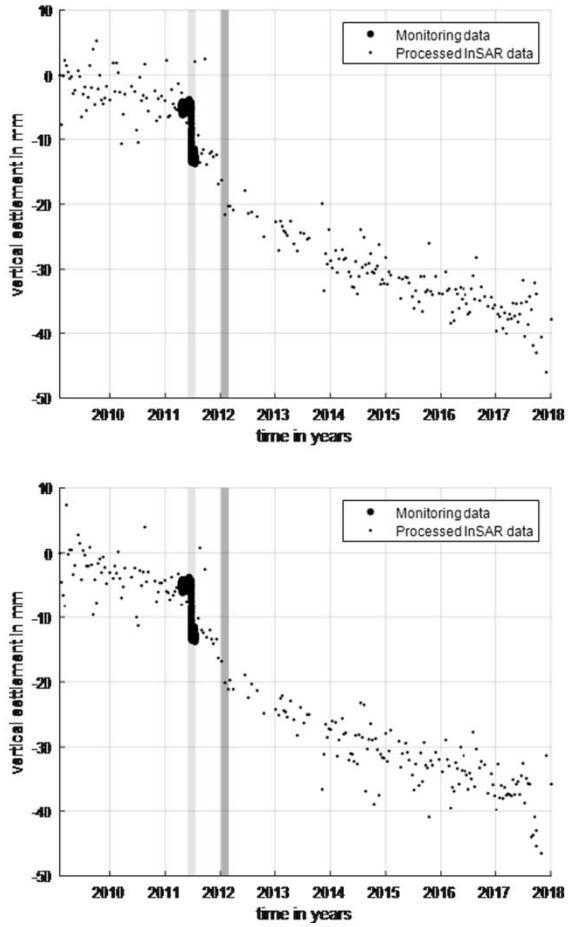

Fig. 16. Verification of the ambiguity level at *Churchilllaan*, point 1 (top) and point 2 (bottom).

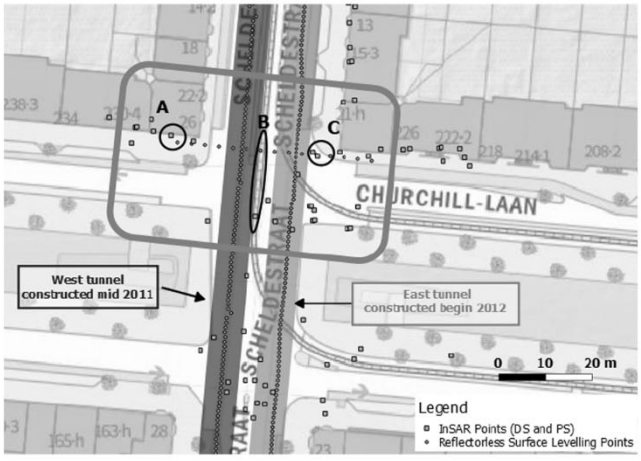

Fig. 17. Location InSAR data and levelling points at *Churchilllaan*.

In Fig. 22 the settlements at the end of each year, starting in 2009, are plotted against the distance to the tunnel axis.

5.3.2. Evaluating the results

Based on Figs. 19 and 22, we conclude that there is a long-term downward trend and that the InSAR data shows a settlement trough that is shaped like a bowl with the largest depth between the tunnels. Therefore, it seems straightforward to deduce that these long-term settlements are a consequence of the tunnel construction. However, the

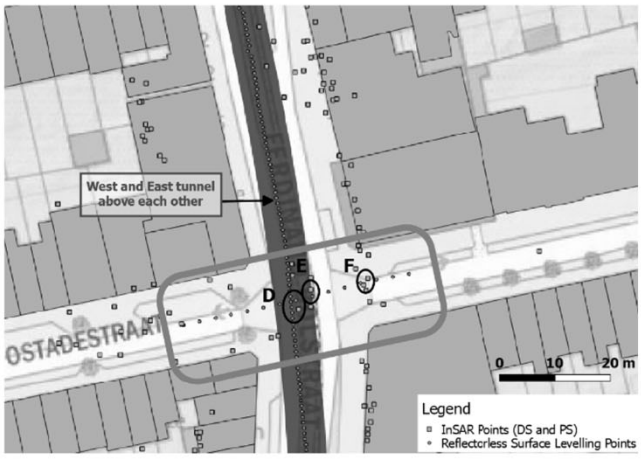

Fig. 18. Location InSAR data and levelling points at *Van Ostadestraat*.

vertical shafts were already excavated in 2010. Therefore, we expect that this is the most likely cause of the increase in settlement velocity starting from the end of 2010, see Section 5.1. Thus, Fig. 19 shows a juxtaposition of settlements due to tunnel construction and settlements due to the vertical shaft excavation. To isolate the long-term effect due to tunnelling only, we also analyze the settlement trough at *Van Ostadestraat*, where there are no vertical shafts, see Fig. 23. We observe that once the settlement trough has occurred, it does not become deeper and wider in time, and the trough settles equally. Moreover, Fig. 24 shows that the settlement trend seems to be linear before and after tunnel construction. We conclude that at the North/South Metro Line, there is no significant long-term effect due to the tunnel construction, and that InSAR is indeed a cost-effective and simple tool to reach this conclusion.

Finally, we also find that the settlement behaviour is not consistent over time. The conventional monitoring data shows heave in February 2012, see Fig. 25. As we suspect that these deviations may be due to atmospheric events, we use meteorological data from the Royal Netherlands Meteorological Institute (KNMI) and find that there was a frost period in February 2012, see Fig. 26.

We conclude that frost may have been a reason for the heave. However, as all total stations are linked to each other and to the reference point, it is also possible that some disturbance happened to the reference point in that period, which could have led to a measurement anomaly. Based on the available information from the conventional monitoring dataset, we cannot draw a unique conclusion. Using the InSAR data to assess this heave, we did not detect heave in point *A* of Fig. 25, even when considering the possibility of ambiguity errors. However, in point *D* of Fig. 25 the InSAR shows a small heave.

6. Discussion

The case of the shield metro tunnel of the North/South Metro Line in Amsterdam shows that the long time period of available SAR data provides unique information about the deformation behaviour prior to construction. The InSAR data reveal that six months prior to the tunnel excavations, an increase in settlement velocity of the surface at *Churchilllaan* occurred. Additionally, the InSAR data showed that the settlement velocity at this location decreased slowly in time but remained at an increased pace for around six years. Future InSAR measurements will tell if this increased settlement velocity is continuing. We speculate that the reason for this increase in settlement is the pumping that took place at the end of 2010 for the construction of the two vertical 30 m deep exit shafts, resulting in a vertical inward movement of the shaft walls, which caused a surface settlement. Also, in general, shafts (like tunnels) are never completely water tight and act as a big vertical well that drains the surrounding soils. This leads to

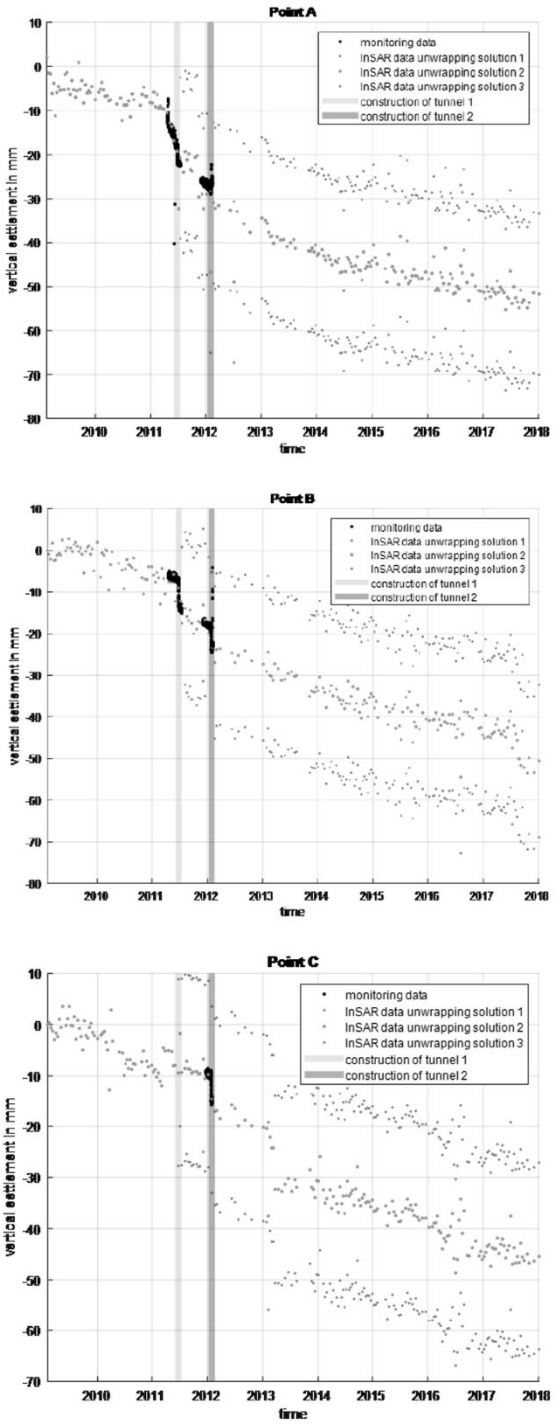

Fig. 19. Comparison InSAR and in-situ data from surface levelling, Points A, B, and C at *Churchilllaan*.

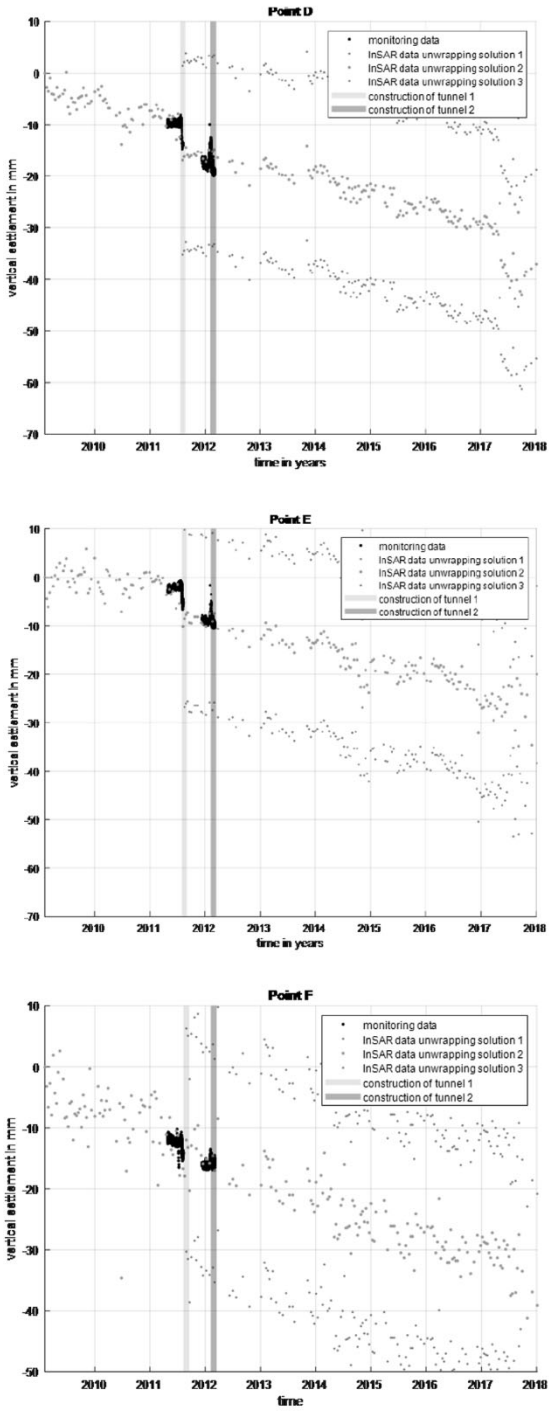

Fig. 20. Comparison InSAR and in-situ data from surface levelling, Points D, E and F at *Van Ostadestraat*.

consolidation during the years after construction, resulting in surface settlements.

7. Conclusions

We evaluated if and how InSAR can be used (i) prior to the tunnel construction to optimise the monitoringsplan, (ii) during construction as a diagnostic tool to detect surface settlements and (iii) after construction as a forensic tool and to monitor the long-term settlements. InSAR provides long times series of deformation, and can be used to map deformations in the past, with SAR data archives going back to 1992. Therefore, it is a very useful tool to perform a baseline assessment *prior* to construction in civil engineering projects. Given the repeat time of the satellite and an extra time latency due to processing of the SAR data, SAR data is not suitable as a real-time warning system *during* construction when immediate action, say, within hours, is needed in case of abrupt settlements. However, due to its high spatial resolution and the availability of long time series, it is a valuable complementary source of information to the conventional monitoring. InSAR provides high-precision monitoring of ground movement over a large area without the need to install instruments on the ground. Also, InSAR provides information about settlement patterns prior to construction when the

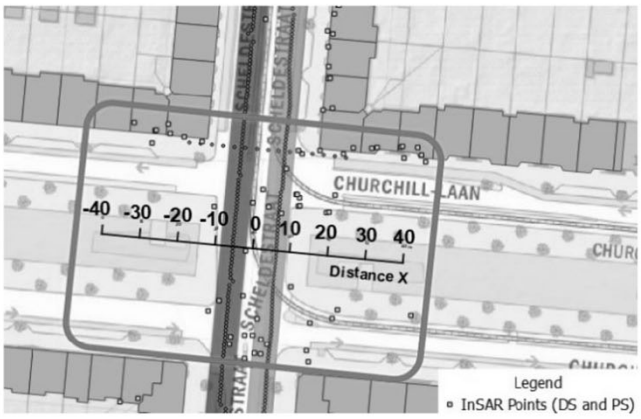

Fig. 21. Selection of InSAR points at *Churchilllaan*.

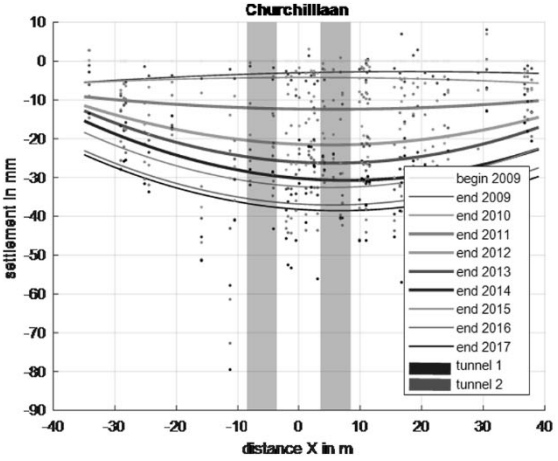

Fig. 22. Vertical settlement of selected InSAR points at *Churchilllaan*.

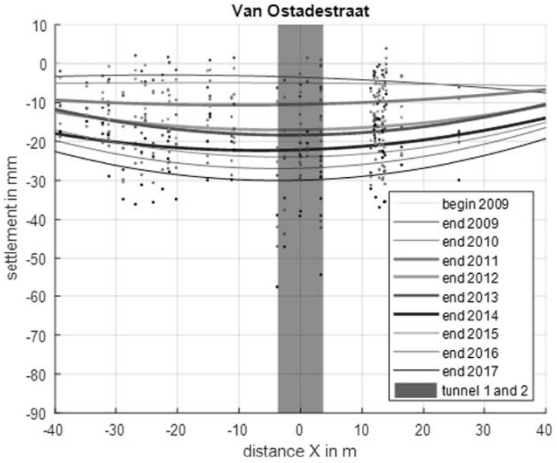

Fig. 23. Vertical settlement of selected InSAR points at *Van Ostadestraat*.

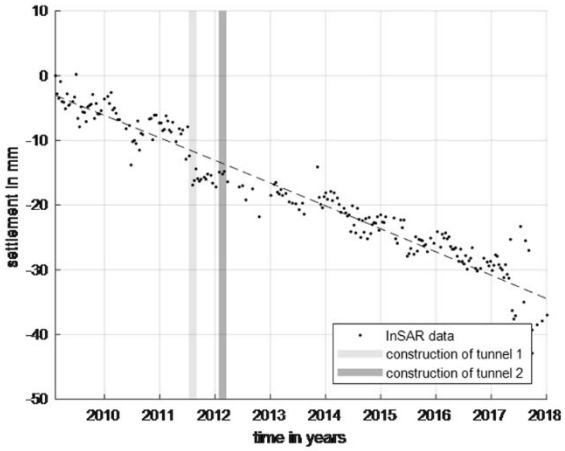

Fig. 24. InSAR point of Fig. 20 at distance $x = 0$.

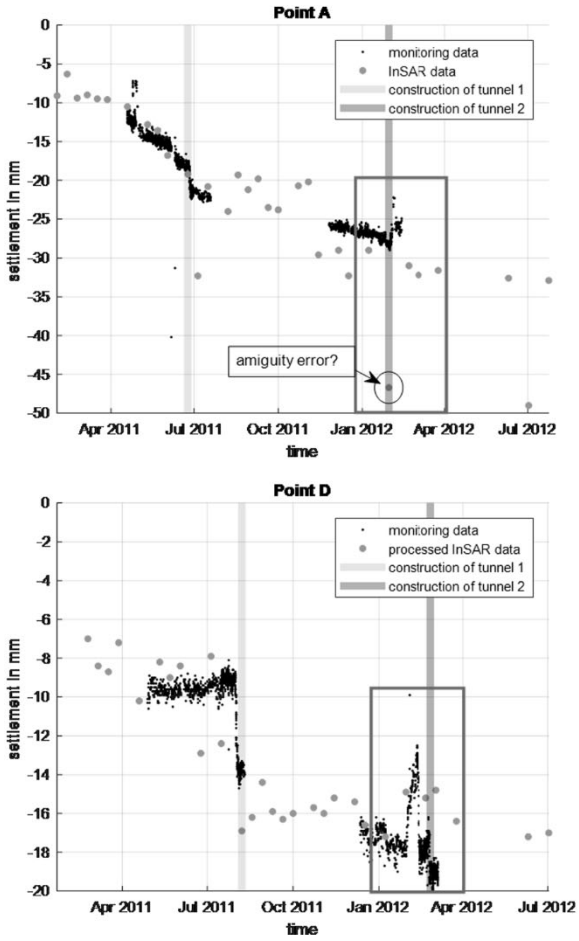

Fig. 25. Detail of points *A* and *D*.

conventional monitoring systems are not installed yet. Finally, InSAR is a useful tool *after* construction to monitor settlements when the conventional monitoring is ceased. It is able to reveal important deformations patters in the years after construction, which will help understand the problem of long-term tunnel settlements better.

Resolving the correct ambiguity level in InSAR data can be challenging, especially in the case of abrupt settlements over short spatial distances with magnitudes close to the wrapping threshold. To retrieve unbiased displacement estimates, prior information regarding the expected settlement is needed. Analytical settlement prediction methods can be used successfully to find the most probable ambiguity level in the InSAR estimates. This way, augmented InSAR can capture the short-term settlements that occur immediately during construction of the shield tunnel. The constraint on the abruptness, steepness, and magnitude of the displacement can be alleviated by having more coherent InSAR scatterers with a shorter repeat cycle. Typically, this favours X-band satellites.

We believe that the proposed methodology to select the most

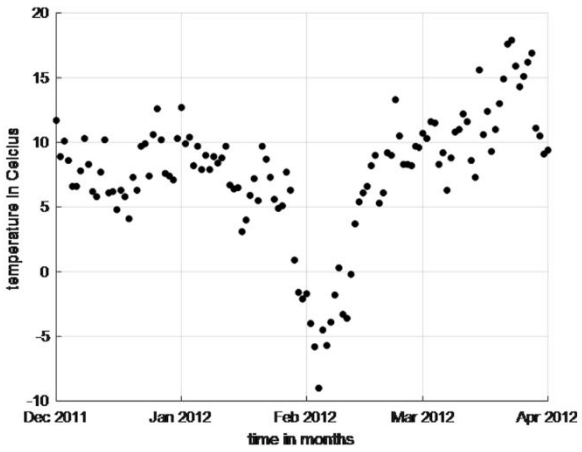

Fig. 26. Temperature in the selected period.

probable ambiguity level can help in the development of a practical tool that is able to quantify and insert the prior information on the displacement dynamics in the InSAR displacement estimation software. And as such, augmented InSAR can be integrated in the monitoring framework of more civil engineering projects.

CRediT authorship contribution statement

Kristina J. Reinders: Conceptualization, Methodology, Investigation, Formal analysis, Visualization, Writing - original draft. **Ramon F. Hanssen:** Conceptualization, Methodology, Writing - review & editing. **Freek J. van Leijen:** Conceptualization, Methodology. **Mandy Korff:** Conceptualization, Methodology.

Declaration of Competing Interest

The authors declare that they have no known competing financial interests or personal relationships that could have appeared to influence the work reported in this paper.

Acknowledgments

The authors wish to thank the Municipality of Amsterdam for providing the surface levelling data and Skygeo for computing and providing the InSAR data.

References

Addenbrooke, T., 1996. Numerical analysis of tunnelling in stiff clay (Ph.D. thesis). Imperial College, London.

Adviesbureau Noord/Zuidlijn, 2014. Oplevering data Monitoring Noord/Zuidlijn. Technical Report L294-13-043-/14-002.928. Adviesbureau Noord/Zuidlijn V.O.F.

Attewell, P.B., Yeates, J., Selby, A.R., 1986. Soil movements induced by tunnelling and their effects on pipelines and structures. Methuen, Inc., New York, NY.

Barla, G., Tamburini, A., Del Conte, S., Giannico, C., 2016. Insar monitoring of tunnel induced ground movements. Geomech. Tunnel. 9, 15–22.

Bischoff, C., Mason, P., Ghail, R., Giannico, C., Ferretti, A., 2019. Monitoring excavation-related ground deformation in london, uk using squeesar. In: Tunnels and Underground Cities. Engineering and Innovation Meet Archaeology, Architecture and Art. CRC Press, pp. 5360–5368.

Bowers, K., Hiller, D., New, B., 1996. Ground movement over three years at the heathrow express rail tunnel. In: Geotechnical Aspects of Underground Construction in Soft Ground-preprint Volume of Proceedings from an International Symposium Held at City University, London, UK, 15–17 APRIL 1996, pp. 647–652.

Broere, W., Festa, D., 2017. Correlation between the kinematics of a tunnel boring machine and the observed soil displacements. Tunn. Undergr. Space Technol. 70, 125–147.

Chang, L., Dollevoet, R.P., Hanssen, R.F., 2018. Monitoring line-infrastructure with multisensor sar interferometry: products and performance assessment metrics. IEEE J. Sel. Top. Appl. Earth Observ. Remote Sens. 11, 1593–1605.

Cook, D., de Nijs, R., Frankenmolen, S., 2007. Amsterdam noord/zuidlijn: Use of background monitoring data prior to construction commencement. In: 7th FMGM 2007: Field Measurements in Geomechanics, pp. 1–12.

Crosetto, M., Monserrat, O., Cuevas-González, M., Devanthéry, N., Crippa, B., 2016. Persistent scatterer interferometry: A review. ISPRS J. Photogramm. Remote Sens. 115, 78–89.

Dheenathayalan, P., Small, D., Schubert, A., Hanssen, R.F., 2016. High-precision positioning of radar scatterers. J. Geodesy 90, 1–20. https://doi.org/10.1007/s00190-015-0883-4.

Elachi, C., 1987. Introduction To The Physics and Techniques of Remote Sensing, second ed. John Wiley & Sons, New York.

Ferretti, A., Prati, C., Rocca, F., 2001. Permanent scatterers in sar interferometry. IEEE Trans. Geosci. Remote Sens. 39, 8–20.

Gabriel, A.K., Goldstein, R.M., Zebker, H.A., 1989. Mapping small elevation changes over large areas: Differential radar interferometry. J. Geophys. Res.: Solid Earth 94, 9183–9191.

Giardina, G., Milillo, P., DeJong, M.J., Perissin, D., Milillo, G., 2019. Evaluation of insar monitoring data for post-tunnelling settlement damage assessment. Struct. Control Health Monit. 26, e2285.

Hanssen, R.F., 2001. Radar Interferometry: Data Interpretation and Error Analysis. Kluwer Academic Publishers, Dordrecht. https://doi.org/10.1007/0-306-47633-9.

Korff, M., Mair, R.J., 2013. Ground displacements related to deep excavation in Amsterdam. 18th International Conference on Soil Mechanics and Geotechnical Engineering: Challenges and Innovations in Geotechnics, ICSMGE 2013.

Macdonald, B., Iannacone, J., Falorni, G., Giannico, C., 2015. Insar-derived time series analysis of tunnel construction-induced ground deformation in urban landscapes. In: Proceedings of the Ninth Symposium on Field Measurements in Geomechanics, Australian Centre for Geomechanics. pp. 315–328.

Maidl, B., Herrenknecht, M., Maidl, U., Wehrmeyer, G., 2013. Mechanised shield tunnelling. John Wiley & Sons.

Mair, R., 2008. Tunnelling and geotechnics: new horizons. Géotechnique 58, 695–736.

Mark, P., Niemeier, W., Schindler, S., Blome, A., Heek, P., Krivenko, A., Ziem, E., 2012. Radarinterferometrie zum setzungsmonitoring beim tunnelbau: Anwendung am beispiel der wehrhahn-linie in düsseldorf. Bautechnik 89, 764–776.

O'Reilly, M.P., New, B., 1982. Settlements above tunnels in the united kingdom-their magnitude and prediction. In: Tunneling'82, London. IMM, pp. 173–181.

Özer, I.E., van Leijen, F.J., Jonkman, S.N., Hanssen, R.F., 2018. Applicability of satellite radar imaging to monitor the conditions of levees. J. Flood Risk Manage. e12509.

Özer, I.E., van Leijen, F.J., Jonkman, S.N., Hanssen, R.F., 2019. Applicability of satellite radar imaging to monitor the conditions of levees. J. Flood Risk Manage. 12, e12509.

Peck, R.B., 1969. Deep excavations and tunneling in soft ground. In: Proc. 7th ICSMFE, 1969, 225–290.

Schindler, S., Hegemann, F., Koch, C., König, M., Mark, P., 2016. Radar interferometry based settlement monitoring in tunnelling: Visualisation and accuracy analyses. Visualiz. Eng. 4, 7.

Schneider, O., Beth, M., Chmelina, K., Rabensteiner, K., Ferretti, A., Giannico, C., Petrat, L., 2015. ITAtech Guidelines for Remote Measurements. Monitoring Systems. Technical Report 3–v2. International Tunnelling and Underground Space Association. https://about.ita-aites.org/wg-committees/itatech/publications/download/1336_33aa8d3d22f1b461ed6c638438e3497c.

Shin, J., Addenbrooke, T., Potts, D., 2002. A numerical study of the effect of groundwater movement on long-term tunnel behaviour. Geotechnique 52, 391–403.

Shirlaw, J., 1995. Observed and calculated pore pressures and deformations induced by an earth balance shield: discussion. Can. Geotech. J. 32, 181–189.

Stallebrass, S., Jovicic, V., Taylor, R., 1994. Short term and long term settlements around a tunnel in stiff clay. In: European conference on numerical methods in geotechnical engineering, pp. 235–240.

Van der Poel, J.T., Gastine, E., Kaalberg, F.J., 2006. Monitoring for construction of the North/South metro line in Amsterdam, The Netherlands. Geotechnical Aspects of Underground Construction in Soft Ground - Proceedings of the 5th International Conference of TC28 of the ISSMGE. https://doi.org/10.1201/noe0415391245.ch103.

Vu, M.N., Broere, W., Bosch, J., 2016. Volume loss in shallow tunnelling. Tunn. Undergr. Space Technol. 59, 77–90.

Wongsaroj, J., Soga, K., Mair, R., 2013. Tunnelling-induced consolidation settlements in london clay. Géotechnique 63, 1103–1115.